frontiers | Frontiers in Physics

TYPE Original Research
PUBLISHED 19 September 2023
DOI 10.3389/fphy.2023.1230004

OPEN ACCESS

EDITED BY
Nirmala Kandadai,
Oregon State University, United States

REVIEWED BY
Patrick Townsend,
ESPOL Polytechnic University, Ecuador
Sohel Rana,
Idaho National Laboratory (DOE), United States
Devyn Duryea,
Oregon State University, Corvallis, United States, in collaboration with reviewer [SR]

*CORRESPONDENCE
Jing Xiao,
xxjjowen@163.com

RECEIVED 27 May 2023
ACCEPTED 21 August 2023
PUBLISHED 19 September 2023

CITATION
Xiao J, Ren G, Guo R, Gan C, Xu Y, Liu Q, Li S, Han D and Lai G (2023), Research on the ablation characteristics of combined lasers for glass fiber reinforced plastic composites.
Front. Phys. 11:1230004.
doi: 10.3389/fphy.2023.1230004

Research on the ablation characteristics of combined lasers for glass fiber reinforced plastic composites

Jing Xiao*, Gang Ren, Rongjun Guo, Chunquan Gan, Yongjun Xu, Quanxi Liu, Shijie Li, Dong Han and Gengxin Lai

Southwest Institute of Technical Physics, Chengdu, China

Glass fiber reinforced plastic (GFRP) composites have been applied to the manufacture of missile shields and unmanned aerial vehicle (UAV) shells. It is of great significance to explore the ablation characteristics of different lasers for these composites. Currently, most existing studies on the ablation characteristics of lasers for Glass fiber reinforced plastic composites are conducted under a single laser output mode, such as continuous wave (CW) laser or pulsed laser. However, the ablation characteristics of combined lasers for Glass fiber reinforced plastic composites have not been clarified. Therefore, the ablation characteristics of single lasers (continuous wave, millisecond (ms) pulsed, or nanosecond (ns) pulsed laser) and combined laser (CW/ms or CW/ns combined pulsed lasers) were investigated by experimental and simulation methods in this study. Additionally, the ablation mechanisms of Glass fiber reinforced plastic under different laser irradiation conditions were compared and analyzed. The results demonstrated that the ablation rates of single lasers for Glass fiber reinforced plastic composites were all within an order of magnitude of 10 μg/J, which was not significantly correlated with the light source system. The ablation efficiency of the single laser was determined by the incident laser energy. The continuous wave laser was found to be the optimal light source for the ablation and destruction of Glass fiber reinforced plastic composites. Nevertheless, there were some obstacles in the ablation process of continuous wave lasers. Applying pulsed lasers during the irradiation of the continuous wave laser may generate a synergistic effect. Under the conditions in this study, the CW/ns pulsed combined laser increased the ablation efficiency by 53.8%.

KEYWORDS

combined laser, glass fiber reinforced plastic composites, ablation characteristics, synergistic damage, thermal-mechanical coupling

1 Introduction

Glass fiber reinforced plastic (GFRP) composites are advantageously characterized by high specific strength, high specific modulus, and favorable electromagnetic properties [1]. These materials are often employed in the military industry to manufacture missile shields and unmanned aerial vehicle (UAV) shells [2]. Therefore, GFRP is one of the typical combat target materials for laser weapons. It would be of enormous significance to explore the damage effect of laser irradiation on GFRP materials. Many scholars from different countries have explored the ablation mechanism and ablation efficiency of different lasers.

In the aspect of the ablation mechanism, He Minbo [3], Li Yadi [4], Shen Pengfei [5], and others studied the pyrolysis phenomenon of epoxy resin under CW laser irradiation, which provided an important reference for the establishment of the ablation mechanism. Huang et al. [6]studied the mechanism of CW lasers in cutting GFRP laminates. They revealed the correlation between ablation and the formation of heat-affected defects. Dittmar [7]and Ma [8] delved into the ablation efficiency of repetitive pulsed lasers for GFRP composites. They confirmed the melting of fibers and resin matrices under the millisecond (ms) and nanosecond (ns) pulse widths and the temperature accumulation under multiple pulses. Charles et al. [9–11] established a calculation model related to the temperature field distribution and interlaminar stress of composite materials under laser irradiation. Peng Guoliang et al. [12, 13] constructed a model related to the energy coupling rate in the laser ablation process. The results indicated that the laser absorption mode was transitioned from bulk absorption to surface absorption with the increase of laser fluence. In the aspect of ablation efficiency, Xu et al. [14] explored the mass loss pattern of multilayer structures caused by laser ablation and mechanical erosion under the subsonic tangential airflow. The experimental results of Chen Bo [15] et al. show that the pyrolysis carbonization of the resin matrix decreased the ablation rate by 24.4%. Liu Ziyu [16] compared the ablation efficiency of ms, microsecond (μs), and ns pulsed lasers for epoxy resin, and found that the ms laser exhibited higher ablation efficiency.

Currently, most studies on the ablation characteristics of lasers for GFRP composites are focused on a single laser, such as a CW laser or pulsed laser. However, there is a lack of systematic comparative studies on the ablation efficiency between CW and pulsed lasers. Additionally, the ablation mechanism and characteristics of composite materials using CW/pulsed combined lasers have not been explored. In this study, the damage characteristics of single lasers (CW, ms, or ns laser) for GFRP composites were unraveled through experimental studies. Moreover, the ablation characteristics of CW/ms and CW/ns combined lasers were further investigated. These studies revealed the mechanism of combined laser synergistic damage. Figure 1 shows a flow chart mapping out the research ideas.

2 Experiment

2.1 Experimental system

As illustrated in Figure 2A, the experimental system was mainly composed of a laser light source system, timing control system, optical system, target, testing equipment, and electron microscope. Among them, the CW laser had an output wavelength of 1.08 μm and a maximum power of 1000 W. The ms pulsed laser and ns pulsed laser both had an output wavelength of 1.06 μm. They had a pulse width of 1 m and 10 ns, respectively, and their single-pulse

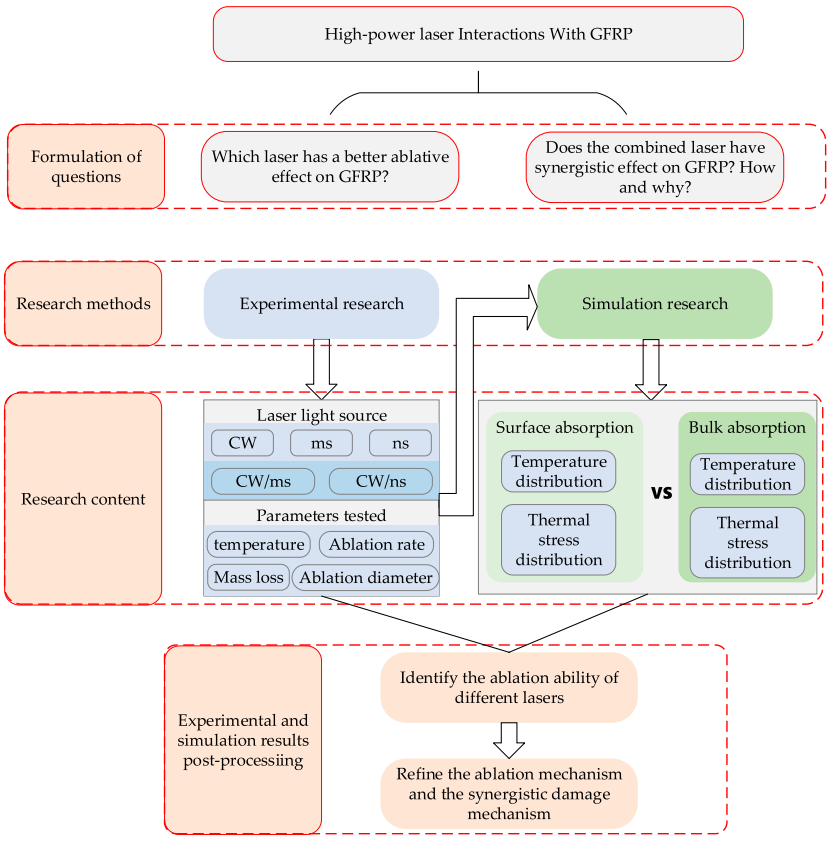

FIGURE 1
Research theory flow chart.

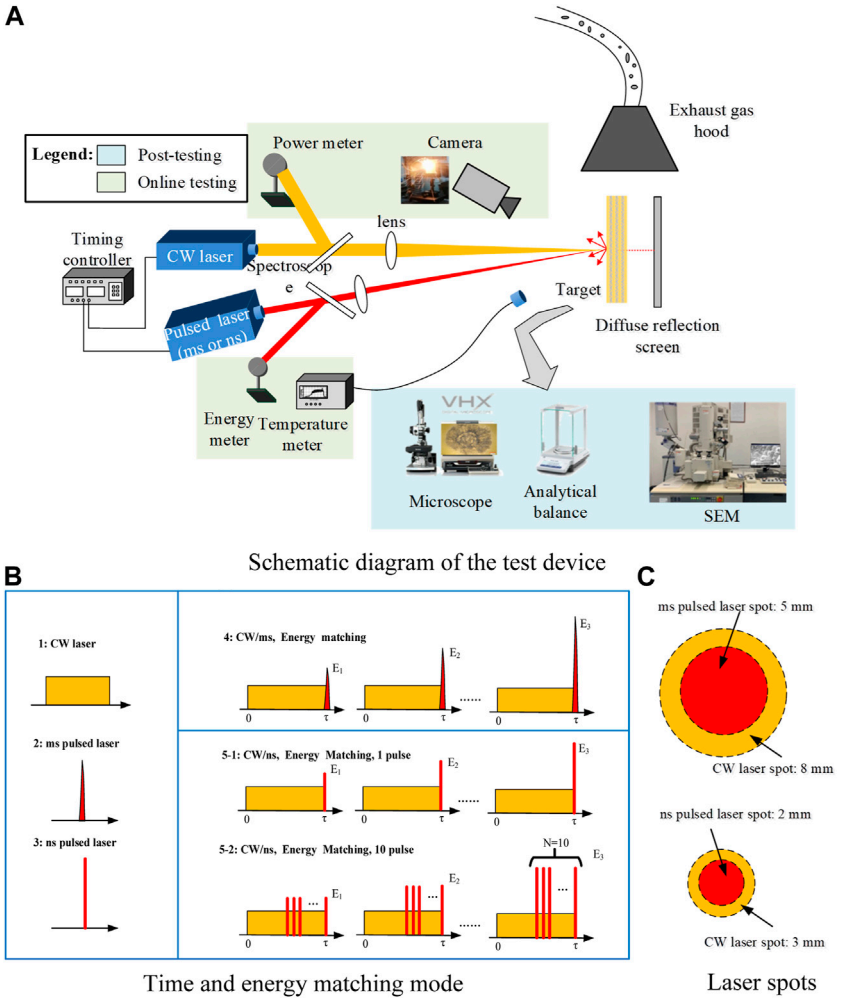

FIGURE 2
Experimental system.

laser energy could be adjusted. The timing control system was utilized to control the laser output mode and adjust the time matching of the combined laser. The laser output modes included CW, pulsed, and combined lasers. As shown in Figure 2B, in the combined laser output mode, the irradiation sequence and time interval of the CW and pulsed lasers could be precisely controlled. The optical system included a focusing lens and a beam splitter, mainly used for spot size control in the two laser beams and monitoring of the laser power/energy. The CW and pulsed lasers were irradiated on the same position of the target at an angle of approximately 8° through the focusing lens. As shown in Figure 2C, when the CW laser and the millisecond pulsed laser were combined, the corresponding spot diameters were 8 mm and 5 mm, respectively; when the CW laser and the nanosecond pulsed laser were combined, the corresponding spot diameters were 3 mm and 2 mm, respectively.

The GFRP plate was adopted as the experimental target with the size of 100 mm × 100 mm×2 mm, with a diffuse reflector placed behind it to observe whether the target was perforated. The test system comprised the laser irradiation process detection and ablation result detection. The former included a power meter, energy meter, spot thermometer, and camera; the latter included an analytical balance and microscope. During laser irradiation, a spot thermometer, KMGA740-L0, was used to measure the temperature change, and a camera was used to record the laser damage process. The mass of the sample before and after laser ablation was measured using an analytical balance (METTLER TOLEDO ME). The damage morphology was observed using an ultra-depth-of-field three-dimensional microscope system (Keyence VHX2000) and scanning electron microscopy (Hitachi).

2.2 Experimental study on the damage characteristics of single lasers for GFRP composites

2.2.1 CW laser

The power density of the CW laser was 750.8 W/cm^2, and the output time of the CW laser was adjusted until the 2 mm target was burned through. Under a high-power CW laser, the temperature of resin matrices rose rapidly, and pyrolysis occurred when the temperature reached 300°C–600°C [17]. Small molecular gas and

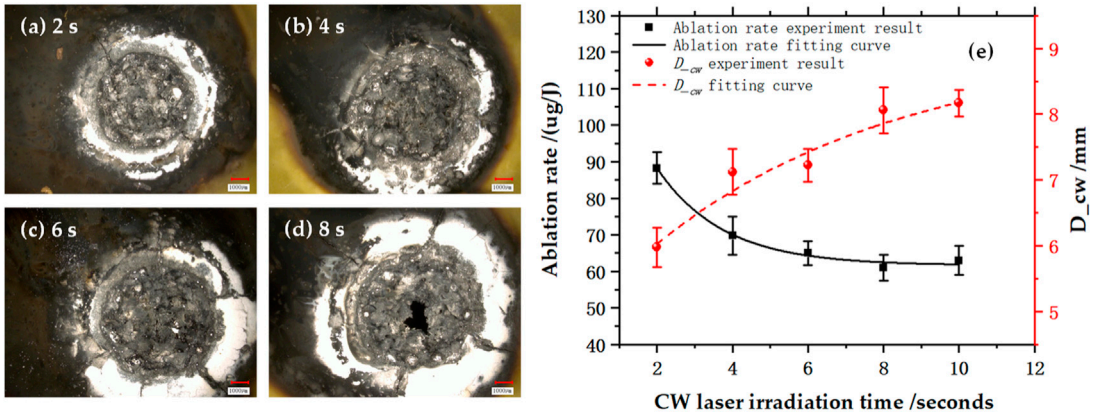

FIGURE 3
Ablation morphology of GFRP composites irradiated by the CW laser. **(A)** Ablation morphology at 2 s; **(B)** 4 s; **(C)** 6 s; **(D)** 8 s; **(E)** Ablation rate and ablation size.

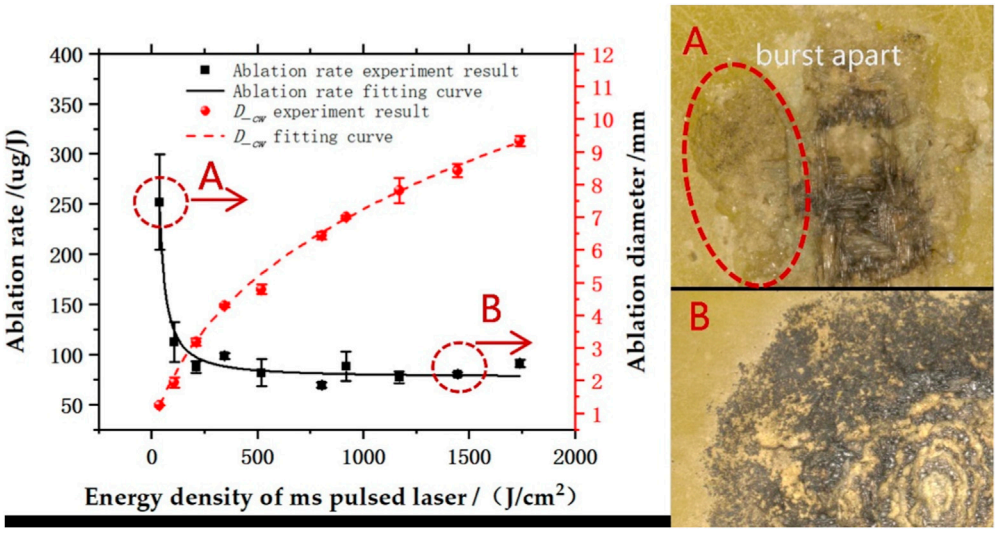

FIGURE 4
The ablation rate of the ms pulsed laser for GFRP composites and the ablation diameter on the upper surface.

loose and porous residual carbon were formed under the action of pyrolysis. They can burn in the air and generate strong black smoke. After the irradiation under CW lasers for about 8 s, the target was perforated completely. Figure 3 shows the change in the ablation morphology, ablation range, and ablation rate on the front surface over different laser irradiation time lengths. Overall, the ablation rate of the irradiation of CW lasers for GFRP targets ranged from 61.0 μg/J to 88.8 μg/J, which was consistent with the test results reported by a study group of the National University of Defense Technology [17]. The experimental results suggested that thermal ablation was the main mechanism of the CW laser for the ablation of GFRP composites. The pyrolysis and combustion of matrix materials occurred simultaneously during the irradiation process.

2.2.2 ms pulsed laser

In the ms pulsed laser ablation experiment, the energy density of the pulsed laser was adjusted until the 2 mm target was burned through. Under the irradiation of ms pulsed laser, the melting and destruction of glass fibers can be observed. The irradiated area was slightly blackened, which can be attributed to the residual carbon generated by the pyrolysis of resin matrices. There was no black smoke in this process, which indicated the absence of combustion. Figure 4 shows the change in the ablation rate of the ms pulsed laser with different energy densities. Overall, the ablation rate of the ms pulsed laser ranged from 77.1 μg/J to 251.9 μg/J. With the increase of the energy density, the ablation rate of the ms pulsed laser for GFRP targets decreased rapidly. When the energy density reached about 200 J/cm^2, the ablation rate was stable in the range of 77.1–98.7 ug/J.

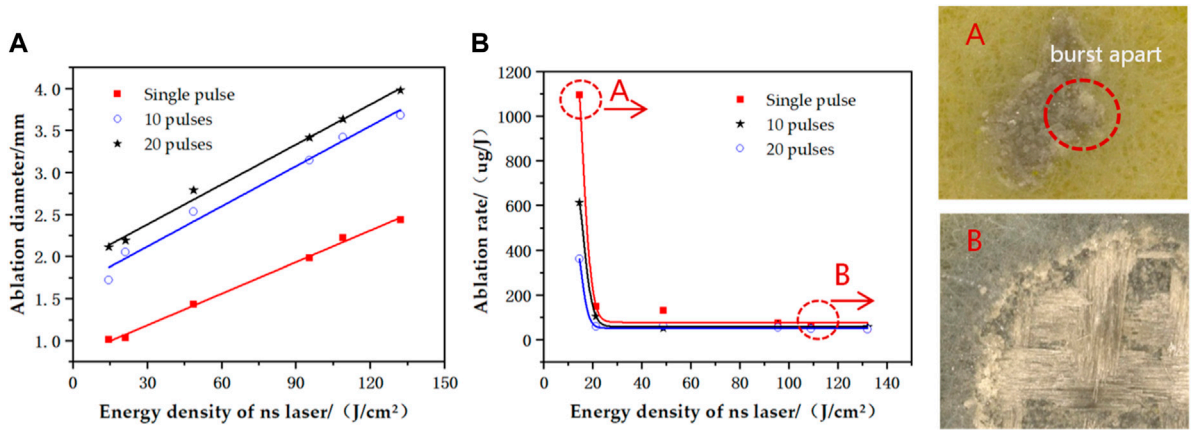

FIGURE 5
The morphology of ablation holes on GFRP composites under the ns pulsed laser. **(A)** Ablation diameter; **(B)** Ablation rate.

There was a significant difference in the ablation rate of the ms pulsed laser between the high-energy density and low-energy density, which can be analyzed from the damage morphology. When the laser energy density was small, the pyrolysis of resin matrices occurred later, accompanied by a low carbonization degree. Under this circumstance, the laser energy was mainly absorbed by the bulk, forming a fracture and causing a large ablation rate, as shown by the ablation morphology corresponding to A in Figure 4. When the laser energy density was high, the pyrolysis of resin matrices occurred early to generate residual carbon. There was a large absorption coefficient of residual carbon to the laser. The energy absorption rapidly transitions from bulk absorption to surface absorption [12, 13]. The mechanical cracking effect was attenuated, and the ablation was mainly caused by a thermal effect, as shown in the ablation morphology corresponding to B in Figure 4.

2.2.3 ns pulsed laser

The ns pulsed ablation experiment was performed under three conditions, including single pulse, 2 Hz/10 pulses, and 2 Hz/20 pulses. The energy density of the ns pulsed laser was adjusted in each experiment by changing the laser voltage. The ablation size and ablation rate were quantitatively measured, as shown in Figure 5.

As shown in Figure 5A, the ablation diameter in the three experiments increased linearly with the energy density. Meanwhile, the larger the number of pulses, the larger the ablation diameter. As shown in Figure 5B, the ablation rate of the ns pulsed laser decreased with the increase of the energy density. Meanwhile, the larger the number of pulses, the lower the ablation rate. Similar to the ms pulsed laser, when the energy density of the ns pulsed laser was low, fracture caused by bulk absorption contributed to a higher ablation rate. When the energy density of the ns pulsed laser reached 21.3 J/cm^2, the ablation rate tended to be stable, ranging from 45.0 μg/J to 60.0 μg/J. Besides, the ablation rate was relatively high under the action of a single ns pulse. That was because a single ns pulse has a limited ablation depth and could only ablate the first layer, epoxy resin, which is easier to be ablated than glass fibers in the inner layers. Under the high-energy density, the ablation efficiency under 10-ns pulses was approximately consistent with that under 20-ns pulses. This indicated that at the repetition rate of 2 Hz, the ablation under the ns laser was relatively independent, and there was almost no mutual enhancement or attenuating effect. Overall, the ablation mechanism under the action of the ns pulsed laser was mainly involved in the pyrolysis of resin matrices and the gasification of glass fibers.

2.3 Experimental study on the damage characteristics of combined lasers for GFRP composites

2.3.1 CW/ms pulsed combined laser

The effect of the ms pulsed laser energy density on the ablation efficiency of the CW/ms combined laser was examined by fixing the irradiation time of the CW laser (4 s, 750.8 W/cm^2). Figure 6 shows the ablation morphology of lasers for composites under different energy densities. The pyrolysis carbonization and white dust formed under intense combustion reactions can be observed in the ablation area. Glass fibers melt in the perforated area on the front surface, followed by the cooling and condensing to form milky white or transparent glass balls. The black residual carbon was relatively small after the pyrolysis of the resin, which indicated that most of the residual carbon was oxidized and ablated.

To illustrate whether the composite laser has enhanced damage efficiency, the most important parameter is the ablation quality. Figure 7 shows the ablation mass under the CW laser alone, the ms laser alone, and the combined laser (CW/ms), as well as the sum of the ablation mass under the CW laser and the ms laser alone (CW + ms). As shown in Figure 7, the ablation mass of the ms pulsed laser alone ranged from 2.4 mg to 16.2 mg. The average ablation rate was 93.7 mg when the CW laser was applied alone for 4 s. The ablation mass was 97.2–105.2 mg under the combined irradiation of CW/ms lasers. This result was equivalent to the sum of the ablation mass under the CW laser and ms laser alone. This indicated that the ablation efficiency of the CW laser combined with a single ms pulsed was only equal to the sum of both, and no synergistic effect can be observed.

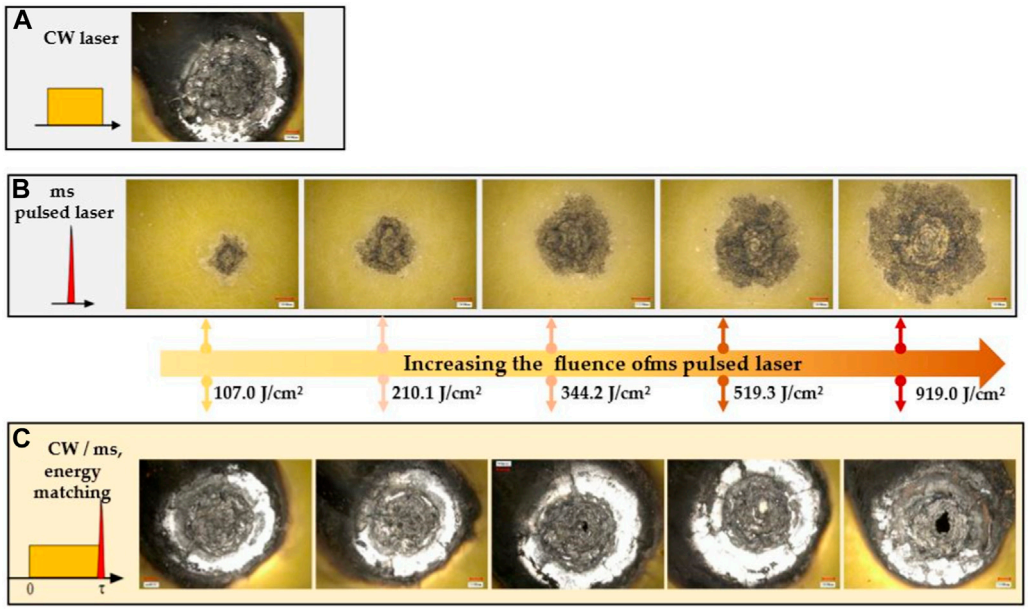

FIGURE 6
The damage morphology of GFRP composites under CW/ms pulsed combined laser.

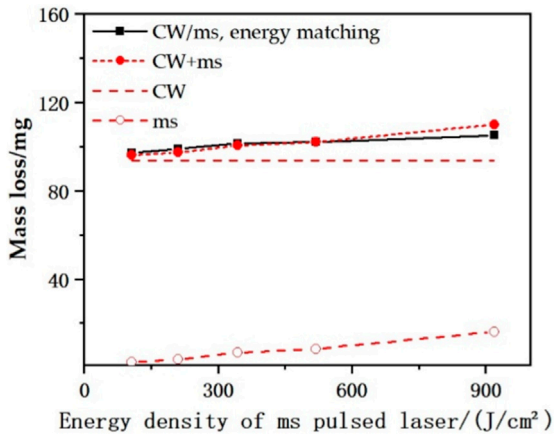

FIGURE 7
The ablation mass of the CW/ms pulsed combined laser for GFRP composites.

2.3.2 CW/ns pulsed combined laser

The effect of the ns pulsed laser energy density and the number of pulses on the ablation efficiency of the CW/ns pulsed combined laser was examined by fixing the irradiation time of the CW laser (10 s, 325.5 W/cm^2).

Figure 8 shows the damage morphology of the CW laser, ns pulsed laser (1 pulse, 10 pulses), and combined laser (CW/ns) for the target. When the CW laser was combined with a single ns pulse, the pyrolysis and combustion products on the front surface splashed out the ablation crater after the pulsed laser was applied. However, there were still many white dust combustion products on the surface. When 10-ns pulses were applied at 5 s, most of the white dust products separated from the target surface, and the ablation crater was exposed and perforated from its center.

Figure 9 shows the ablation quality of the target material by the composite laser in the two proportioning modes of CW/1-ns pulses and CW/10-ns pulses. The blue region stands for the increment of the ablation mass of the combined laser compared with the sum of the ablation mass under the CW laser alone and the ns pulsed laser alone. Compared with the single laser irradiation, the CW/ns pulsed combined laser has an enhanced ablation effect. Under the laser parameters in this experiment, the ablation mass of the CW/ns pulsed combined lasers under 1-ns pulses increased by 7.3% at the maximum; The ablation mass of the CW/ns pulsed combined lasers under 10-ns pulses increased by 53.8%.

3 Analysis

3.1 Comparative analysis of ablation characteristics between the single and combined lasers

In this paper, the destructive ability of laser on glass fiber/epoxy composites is mainly studied, so the experimental results of low energy density and surface resin ablation are not considered. Table 1 lists the ablation rates of three single lasers and two composite lasers at higher power/energy densities.

The results indicated that there was no significant difference in the ablation efficiency of the CW laser, ms pulsed laser, and ns pulsed laser for GFRP composites, which were in the order of magnitude of 10 μg/J (Table 1). And, the ablation damage under the thermal action was the main damage mechanism. Specifically,

10.3389/fphy.2023.1230004

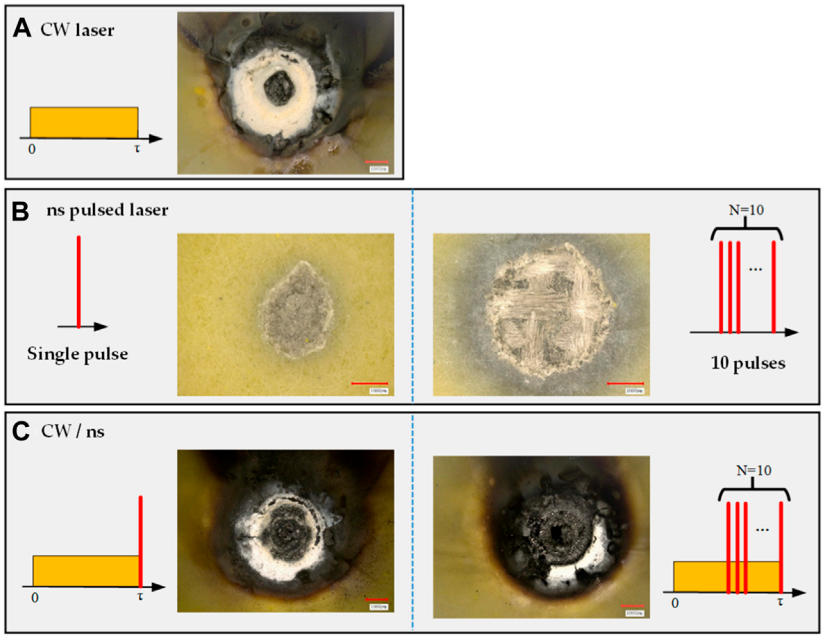

FIGURE 8
The ablation morphology of CW/ns combined lasers.

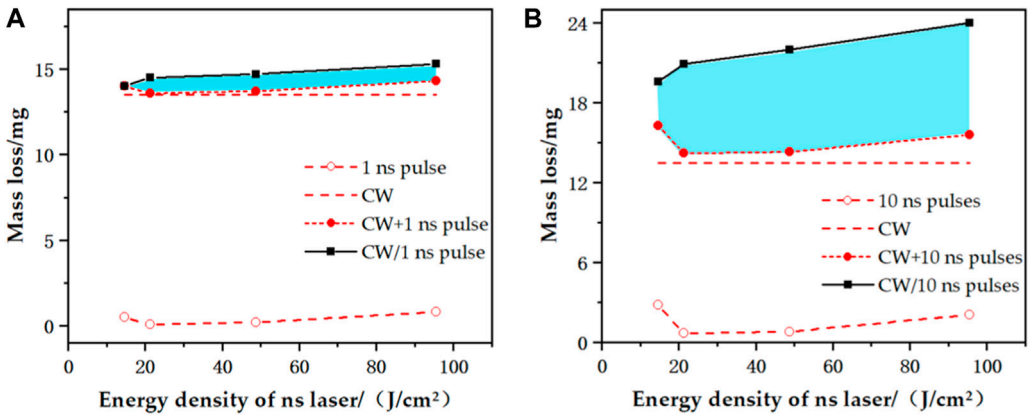

FIGURE 9
Increase of the ablation mass. **(A)** CW/1 ns pulse; **(B)** CW/10 ns pulse.

TABLE 1 Ablation efficiency of multi-system lasers for GFRP composites.

Laser system	Ablation ability
CW laser	Ablation rate: 61.0–88.8 μg/J
ms pulse laser	Ablation rate: 77.1–98.7 μg/J
ns pulse laser	Ablation rate: 45.0–60.0 μg/J
CW/ms composite laser	The ablation mass is the superposition of CW and ms pulse, without mutual reinforcement effect
CW/ns composite laser	CW/1 ns pulse: the ablation quality has been improved by 7.3%; CW/10 ns pulses: the ablation quality has been improved by 53.8%。

the ablation mass of lasers for GFRP composites was determined by the laser input energy. The pulsed laser and CW laser were characterized by long action time and large input energy. Compared with a pulsed laser, a CW laser has the advantages of long irradiation time and large input energy which make it to be the best light source for damaging GFRP composites.

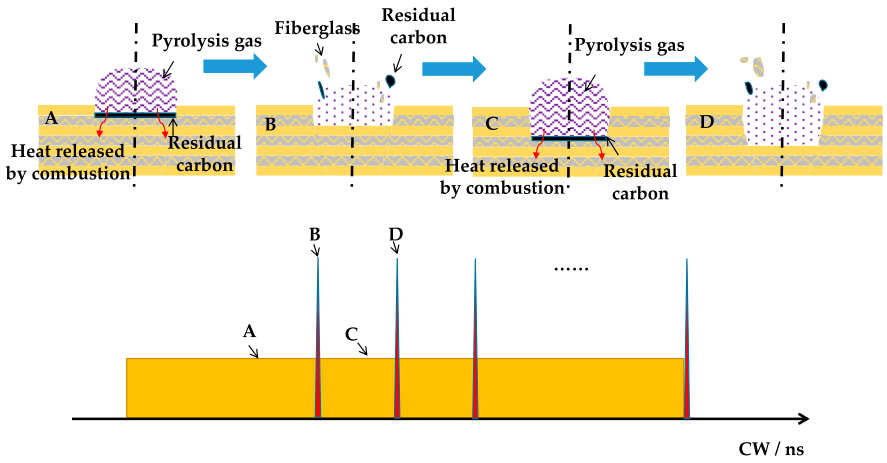

FIGURE 10
The mechanical denudation mechanism model of combined lasers.

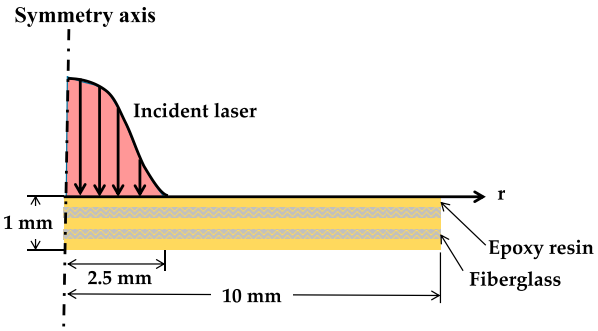

FIGURE 11
Two-dimensional axisymmetric calculation model.

Combustion occurred in the irradiation of the CW laser. Therefore, the input energy was composed of the laser energy and the heat released by combustion. However, the ablation rate of the CW laser was only 61.0–88.8 μg/J. Hence, the CW laser was not superior to the pulsed light source without combustion. This result was even slightly lower than that of the ms pulsed laser. This indicated that there were obstacles in the ablation process of CW lasers, which can be attributed to two factors. Firstly, the pyrolysis and combustion of the resin matrix under CW laser irradiation was not sufficient, accompanied by strong black smoke. According to the shape of the damage, there is a large amount of residual carbon remaining. This suggested that the chemical energy of resin matrices cannot be fully converted into heat energy to further enhance combustion. Secondly, the existence of glass fibers and SiC [18] formed by the reaction between glass fibers and residual carbon hindered further combustion.

Compared with the irradiation under the CW laser or the pulsed laser alone, CW/ms pulsed combined laser cannot generate synergistic effects under the laser parameters of this study. CW/1-ns pulsed combined laser efficiency is increased by 7.3%. The synergistic effect was not obvious under the irradiation of CW and single-pulsed combined laser. Mainly because the pulsed laser is not applied at the right time. The pulsed laser was applied at the end of the irradiation with the CW laser. After the glass fiber melt and SiC were denuded by the pulsed laser, no CW laser was applied, thus failing to realize synergistic effects. The ablation efficiency of CW/10-ns pulsed combined laser is increased by 53.8%, exhibiting an obvious synergistic effect. This can be explained that the pulsed laser can denudate glass fibers and SiC, and the repetition mode of action allows the process of ablation to be repeated, as shown in Figure 10.

3.2 Comparative analysis of bulk absorption and surface absorption

In the pulsed laser ablation experiment, there was a significant difference in the ablation efficiency of pulsed lasers between the high- and low-energy densities. From the perspective of damage morphology, carbonization became more obvious with the increase of energy density, the preliminary analysis is caused by the rapid conversion of the material's absorption of the laser from bulk absorption to surface absorption. To verify this conjecture, a simplified two-dimensional axisymmetric calculation model was established, as shown in Figure 11. The thickness of the target was 1 mm, including 5 layers from the top to the bottom. The top layer is epoxy resin, then epoxy resin and glass fiber are arranged in layers, each layer is 0.2 mm thick. The ms laser (Gaussian beam, with a spot radius of 2.5 mm) was applied on the upper surface of the model. The stress of materials was analyzed under bulk absorption and surface absorption. The bulk absorption was calculated under the energy density of 40 J/cm^2; while the surface absorption was calculated under the energy density of 500 J/cm^2. The material parameters are listed in Table 2. The radial strength of GFRP composites can be calculated as [19].

$$\sigma_i = \sigma_i^0 \cdot f \cdot \left(\exp\left(-b\frac{T}{T_0} - 1 + \beta(T) \right) + (1-f)\cdot d \right), i = r, z \quad (1)$$

where, σ_i^0 is the strength of the original material at normal temperature; $\beta(T)$ is the creep term, which can be ignored in the intense laser irradiation due to the short action time; T_0 is the room temperature (300 K); b and d are material constants. For the radial strength of GFRP composites, σ_r^0 = 200 MPa, b = 0.3, and d = 0; For

TABLE 2 Parameters of GFRP composites [10, 14, 16].

Material	Elastic modulus (N/m^2)	Coefficient of thermal expansion (K^{-1})	Poisson ratio	Thermal conductivity (W/m·K)	Absorption coefficient (m^{-1})	Transmittance
Epoxy resin	1.0×10^{10}	6.7×10^{-6}	0.307	0.3	$\begin{cases} 360, T<380K \\ \left[360-\frac{160}{140}(T-380)\right], 380K\le T\le 520K \\ 200, T>380K \end{cases}$	0.7
Glass fiber	7.6×10^{9}	4.8×10^{-6}	0.25	0.01–0.05	10	0.9993

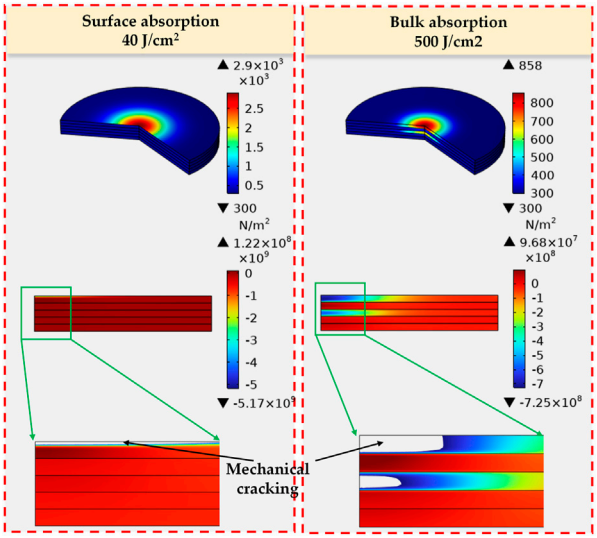

FIGURE 12
(A) Temperature distribution; **(B)** stress distribution; and **(C)** mechanical cracking range under surface absorption and bulk absorption.

the thickness direction of GFRP composites, σ_z^0 = 10 MPa, b = 0.7, and d = 0.1.

Figures 12A, B show the temperature distribution and stress distribution after ms laser irradiation under two absorption modes. Under surface absorption, the material temperature and thermal stress were high, but the heat-affected area was small. Under bulk absorption, the material temperature and thermal stress were low, but the heat-affected area was large. According to the calculation results of the temperature field in Figure 12A, the radial strength of GFRP under surface absorption and bulk absorption can be calculated to be 57.2 MPa and 7.4 MPa, respectively, based on Formula (1). Figure 12C shows the area above the strength of the material, namely the mechanical cracking range caused by thermal stress, as shown in the white area in the figure. It can be seen that there was a large cracking range under bulk absorption, which contributed to a higher ablation rate. The computational model results are consistent with the experimental results, revealing the change mechanism of the ablation rate at different fluences.

4 Conclusion

In order to assess and find a laser light source with better ablation efficiency for laser weapons and laser processing, selecting GFRP composites as the research object, the ablation characteristics of single lasers (CW, ms, or ns laser) and combined lasers (CW/ms or CW/ns combined lasers) were investigated. The results demonstrated that: 1) As for the damage mechanism, the thermal ablation was the main ablation mechanism of the CW laser for GFRP composites, accompanied by pyrolysis and combustion of matrix materials. The ablation mechanism of the ms laser was mainly involved in resin matrix pyrolysis and glass fiber melting, regardless of the combustion of pyrolysis products. Besides, thermal stress cracking damage caused by bulk absorption may be induced under a low power density of the ms pulsed laser. In contrast, the ablation mechanism of the ns laser was mainly involved in resin matrix pyrolysis and glass fiber gasification, regardless of the combustion of pyrolysis products and melting/solidification of glass fibers. 2) As for optimizing laser light sources, the CW laser was the optimal light source for the damage of GFRP composites. However, the ablation efficiency of the CW laser was limited when it was used alone due to the insufficient pyrolysis and combustion of resin matrices. These glass fibers and relevant reactions with residual carbon generated SiC, which hindered further combustion. 3) As for the ablation efficiency enhancement, an enhanced synergistic effect was observed when the pulsed laser was applied in the repetition frequency mode during CW laser irradiation, and the CW/ns pulsed combined laser increased the ablation efficiency by 53.8%.

Through this article, the ablation mechanism for GFRP of different lasers has been refined. Meanwhile, the knowledge gap on the mechanism and ablation ability of CW/ms and CW/ns combined lasers have been explored. The results can be applied in the military and industrial to optimize the laser light source for better efficiency.

Data availability statement

The original contributions presented in the study are included in the article/supplementary material, further inquiries can be directed to the corresponding author.

Author contributions

JX is the main author of this article, who designed the experiment to complete the research and conducted theoretical analysis. RG is the secondary author of the article, who assisted X in completing the experiment and conducting theoretical analysis. GR and CG provided guidance for the study. JX, SL, QL, DH, and GL

provided valuable suggestions for the study. All authors contributed to the article and approved the submitted version.

Conflict of interest

The authors declare that the research was conducted in the absence of any commercial or financial relationships that could be construed as a potential conflict of interest.

Publisher's note

References

1. Du S. Advanced composite materials and aerospace [J]. *J Compos Mater* (2007)(01) 1–12. doi:10.13801/j.cnki.fhclxb.2007.01.001

2. Chen S. Application and research of composite materials on drones [J]. *Aircraft Des* (2003)(03) 26–30. doi:10.19555/j.cnki.1673-4599.2003.03.006

3. He M, Ma Z, Liu W. Study on the pyrolysis of carbon fiber epoxy resin composites under continuous laser irradiation [J]. *Mod Appl Phys* (2016) 7(01):48–52. doi:10.3969/j.issn.2095-6223.2016.01.009

4. Li Y, Wu P, Ma X. Experimental study on continuous laser ablation of carbon fiber/epoxy resin composite laminates [J]. *Fiber Compos Mater* (2010) 27(02):21–4. doi:10.3969/j.issn.1003-6423.2010.02.006

5. Shen P. Study on the damage mechanism of multilayer composite materials under high power laser irradiation [D]. *Donghua Univ* (2022). doi:10.27012/d.cnki.gdhuu.2022.000299

6. Huang S, Fu Z, Liu C, Wang C. Interactional relations between ablation and heat affected zone (HAZ) in laser cutting of glass fiber reinforced polymer (GFRP) composite by fiber laser. *Opt Laser Technol* (2023) 158:108796. doi:10.1016/j.optlastec.2022.108796

7. Dittmar H, Gäbler F, Stute U. UV-Laser ablation of fibre reinforced composites with ns-pulses. *Phys Proced* (2013) 41:266–75. doi:10.1016/j.phpro.2013.03.078

8. Ma Y, Xin C, Zhang W, Jin G. Experimental study of plasma plume analysis of long pulse laser irradiates CFRP and GFRP composite materials. *[J] Crystals* (2021) 11(5): 545. doi:10.3390/cryst11050545

9. Boley CD, Rubenchik AM. Modeling of laser interactions with composite materials. *Appl Opt* (2013) 52(14):3329–37. doi:10.1364/ao.52.003329

10. Gay E, Berthe L, Boustie M, Arrigoni M, Trombini M. Study of the response of CFRP composite laminates to a laser-induced shock. *Composites B: Eng* (2014) 64: 108–15. doi:10.1016/j.compositesb.2014.04.004

11. Liu W, Liu YW. Numerical simulation of microwave transmission attenuation induced by laser ablation carbonization of FRP [J]. *Infrared Laser Eng* (2021) 50(12): 20210137–1. doi:10.3788/IRLA20210137

12. Peng G, Du T, Liu F, Zhang X. Simulation of energy coupling rate of laser ablation glass fiber/epoxy resin composites [J]. *China Laser* (2014) 41(2):0203001. doi:10.3788/IRLA20210137

13. Peng G, Zhnag XG. Study on mechanical erosion of laser irradiated glass fiber/epoxy resin composite materials [J]. *China Laser* (2015) 42(1).

14. Xu S, Nan P, Shen Z, Zewen L, Han B, Pan Y, et al. Mechanical erosion effect of continuous-wave laser ablation of GFRP under subsonic airflow; sixth symposium on novel optoelectronic detection Technology and applications. *SPIE* (2020) 11455:7. doi:10.1117/12.2564705

15. Chen B, Wan H, Mu J, Abrams B, Shaw GM. NTD prevalences in central California before and after folic acid fortification. *Intense Laser Part Beam* (2008) 82(04):547–52. doi:10.1002/bdra.20466

16. Liu Z. Analysis of the process of pulse laser damage to epoxy resin [D]. *Changchun Univ Sci Technol* (2014).

17. Chen M. *Study on the irradiation effect of laser on fiber reinforced resin matrix composites under tangential airflow [D]*. Changsha: National University of Defense Science and Technology (2012).

18. Xu S. *Study on the ablation characteristics of glass fiber reinforced resin matrix composites under tangential air flow under continuous laser irradiation [D]*. Nanjing: Nanjing University of Science and Technology (2020).

19. Dimitrienko YI, Dimitrienko YI. *Mathematical model of ablative composites[M]*. Springer Netherlands (2016).